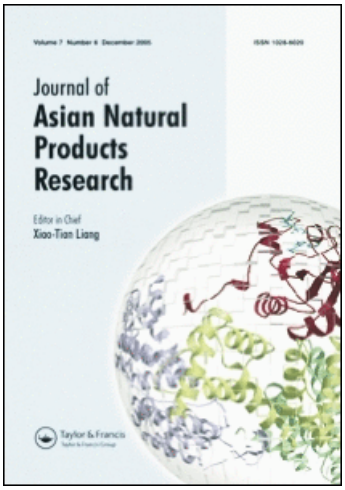

Journal of Asian Natural Products Research
Publication details, including instructions for authors and subscription information:
http://www.informaworld.com/smpp/title~content=t713454007

Tephrosin-induced autophagic cell death in A549 non-small cell lung cancer cells

Jing Li[a]; Xiao-Lu Wang[a]; Yu-Chun Fang[a]; Chang-Yun Wang[a]
[a] Key Laboratory of Marine Drugs, Ministry of Education, School of Medicine and Pharmacy, Ocean University of China, Qingdao, China

Online publication date: 08 November 2010

To cite this Article Li, Jing , Wang, Xiao-Lu , Fang, Yu-Chun and Wang, Chang-Yun(2010) 'Tephrosin-induced autophagic cell death in A549 non-small cell lung cancer cells', Journal of Asian Natural Products Research, 12: 11, 992 — 1000
To link to this Article: DOI: 10.1080/10286020.2010.513034
URL: http://dx.doi.org/10.1080/10286020.2010.513034

Journal of Asian Natural Products Research
Vol. 12, No. 11, November 2010, 992–1000

Tephrosin-induced autophagic cell death in A549 non-small cell lung cancer cells

Jing Li, Xiao-Lu Wang, Yu-Chun Fang and Chang-Yun Wang*

Key Laboratory of Marine Drugs, Ministry of Education, School of Medicine and Pharmacy, Ocean University of China, Qingdao 266003, China

(*Received 15 March 2010; final version received 31 July 2010*)

Anticancer effect of tephrosin (**1**) has been documented; however, the molecular mechanisms underlying the cytotoxicity of tephrosin in cancer cells remain unclear. In the present paper, the proliferation inhibition rate of several cancer cells was tested using the MTT assay; cell cycle, reactive oxygen species (ROS), and mitochondrial membrane potential (MMP) were determined by flow cytometry; poly(ADP-ribose) polymerase (PARP) cleavage and heat shock protein 90 (Hsp90) expression were evaluated by Western blotting; autophagy was examined by confocal microscopy and light chain 3 (LC3) conversion assay. The results showed that exposure of the cells to tephrosin induced significant proliferation inhibition in a dose-dependent manner, especially on A549 with G_2/M being arrested. Tephrosin was not found to induce cell apoptosis as PARP cleavage was not detected after 24 h treatment, but the formation of acidic vesicular organelle of autophagy character was found, and autophagy was further confirmed by the increase in the ratio of LC3-II to LC3-I. It was observed that tephrosin induced ROS generation and Hsp90 expression inhibition. These results indicate that tephrosin induces A549 cancer cell death via the autophagy pathway, and the roles of ROS generation and Hsp90 expression inhibition in this process need further study in the future.

Keywords: tephrosin; autophagy; ROS; Hsp90

1. Introduction

Deguelin and tephrosin, two rotenoid isoflavonoids with insecticidal activity, were mainly isolated and identified from the plants of the genus *Derris*. In recent years, deguelin has been well studied for its antitumor activity and has proven to be a promising chemopreventive and therapeutic agent to treat diverse types of cancer [1]. Tephrosin was first separated by high-performance liquid chromatography in 1975. Later research results showed that tephrosin available in a few plants also had potential antitumor activity [2]. However, the anticancer mechanisms of tephrosin have not been defined when compared with deguelin.

We obtained pure tephrosin (purity $>99.2\%$) from the roots of *Derris trifoliate* Lour. by bioassay-guided fractionation in our effort to search for novel chemopreventive agents (**1**, Figure 1). In this paper, we provide evidences that tephrosin can induce several cancer cells to death, especially to autophagy in the non-small cell lung cancer cell line A549 accompanied by reactive oxygen species (ROS) generation and heat shock protein 90 (Hsp90) expression inhibition.

*Corresponding author. Email: changyun@ouc.edu.cn

ISSN 1028-6020 print/ISSN 1477-2213 online

DOI: 10.1080/10286020.2010.513034
http://www.informaworld.com

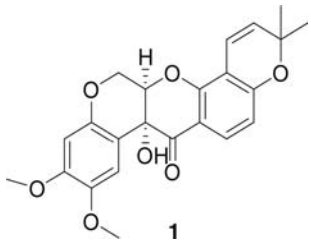

Figure 1. Structure of tephrosin (**1**).

2. Results and discussion

2.1 Cytotoxicity of 1 against different cancer cell lines

The characterization of the effects of **1** on the growth of different cancer cell lines was performed at different concentrations of **1** for 48 h. The results showed that **1** resulted in the dose-dependent decrease in viability in cell lines P388, Bel7402, and A549, compared with the control (Figure 2). A549 was more sensitive to **1** than other cells, with an inhibition rate of 44.4% at 0.1 μg/ml.

2.2 Effect of 1 on cell cycle progression

To elucidate the mechanisms responsible for the reduction of cell number by **1**, we first examined the possible changes in cell cycle progression. Figure 3 shows the distribution of A549 cells in the different cell cycle phases after 12 h of **1** treatment. A significant increase in the percentage of cells in the G_2/M phase was observed, accompanied by a concomitant decrease in the G_0/G_1 phase.

2.3 Effect of 1 on the cleaved fragments of PARP

Arrest of the cell cycle generally leads to cell apoptosis [3]. Therefore, we examined the effect of **1** on the cleaved fragments of poly(ADP-ribose) polymerase (PARP), which acts as a marker for apoptosis. As illustrated in Figure 4, our data showed that **1** did not significantly induce the cleaved fragments of PARP protein. Taking the results of cell cycle progression assay into consideration that the population of the sub-G_1 phase was not detected, which denotes the occurrence of apoptosis, we suggested that arresting of the cell cycle by **1** was probably not followed by apoptosis in A549 cells.

2.4 Effect of 1 on the production of ROS

The production of intracellular ROS in A549 cells after the treatment with **1** for 2 and 24 h was measured by flow cytometry. The incubation of cells with **1** induced a significant increase in intracellular ROS

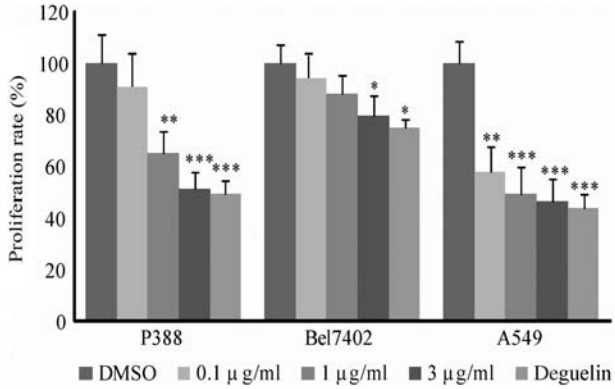

Figure 2. Tephrosin (**1**) caused a significant decrease in viability in cell lines P388, Bel7402, and A549 when compared with the control. Each column indicated mean ± SD of three independent experiments. $*P < 0.05$, $**P < 0.01$, $***P < 0.001$ vs. DMSO group.

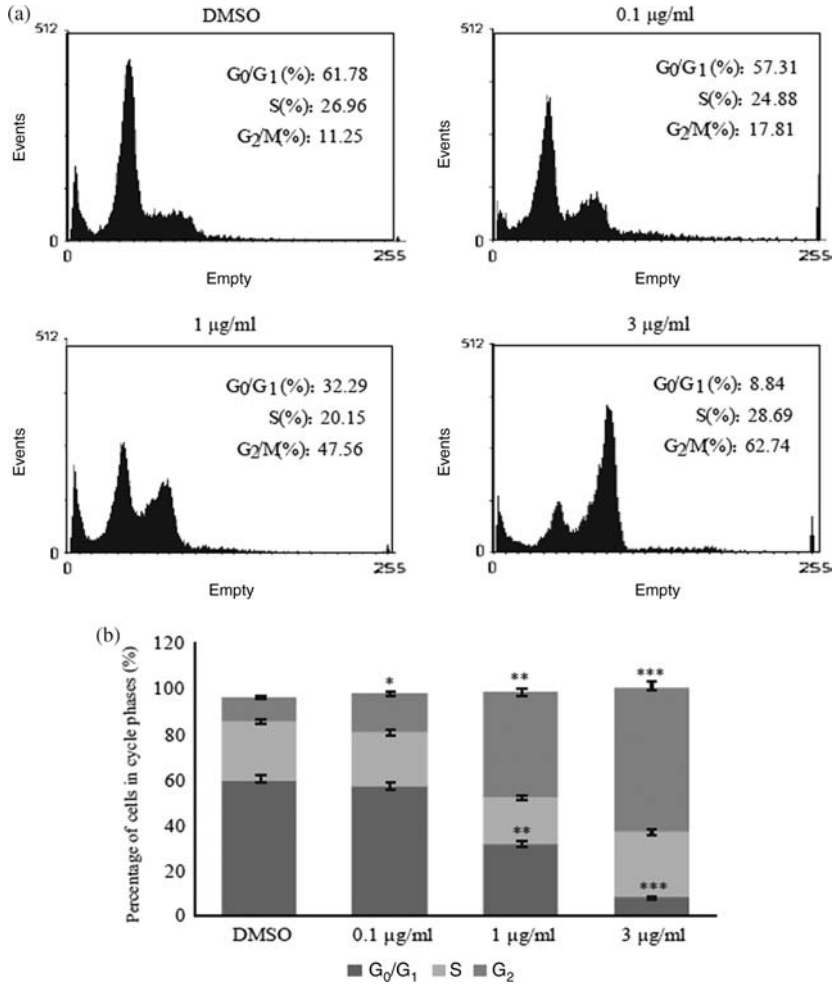

Figure 3. Effect of tephrosin (**1**) on cell cycle progression in A549 cancer cells. (a) Representative flow cytometric analyses. (b) Statistical analyses. The values were the means ± SD, $n = 3$. $*P < 0.05$, $**P < 0.01$, $***P < 0.001$ vs. DMSO group.

production in a dose-dependent manner, as shown in Figure 5, by the increased fluorescence intensity with respect to the vehicle alone.

2.5 Introduction of autophagy by 1 in A549 cancer cells

Because ROS have been involved in autophagy [4,5], we studied whether ROS mediate autophagic cell death induced by **1**. Autophagy was characterized by the formation of acidic vesicular organelle (AVOs) [6,7]. AVOs were analyzed by confocal microscopy after the cells were stained with acridine orange (AO): the cytoplasm and the nucleolus fluoresce bright green and dim red, whereas AVOs fluoresce bright red [8]. In this study, we found that **1** significantly induced AVO formation in A549 cancer cells with bright red fluorescence around the cell nucleus (Figure 6(a)). Tracking the conversion of light chain 3-I (LC3-I) to LC3-II is

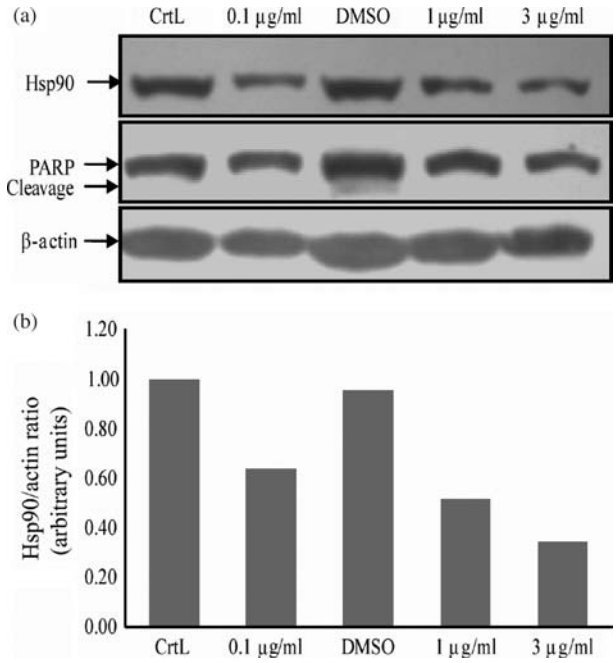

Figure 4. Effects of tephrosin (**1**) on the PARP protein cleavage and expression of Hsp90 in A549 cancer cells treated for 24 h. (a) Representative Western blotting analysis of three independent experiments. (b) Densitometric analyses of the ratio of Hsp90 to actin.

indicative of autophagic activity; in the further study, we monitored an increase in the LC3-II:LC3-I ratio and confirmed the effect of **1** on autophagy in A549 cells (Figure 6(b) and (c)).

2.6 Reduction effect of 1 on Hsp90 expression

Hsp90 is responsible for the conformational maturation of nascent polypeptides and the renaturation of denatured

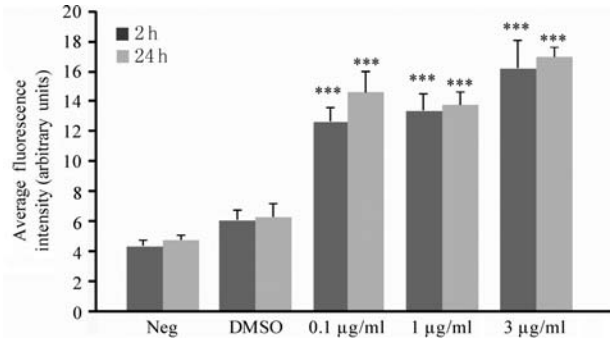

Figure 5. The incubation of A549 cells with tephrosin (**1**) induced a significant increase in intracellular ROS production. Data are average values of relative fluorescence of the peak from one representative experiment of three experiments. 'Neg' denotes the internal negative control that A549 cells incubated with the vehicle in the absence of DCFH-DA. Representative flow cytometric analyses. The values were the means ± SD, $n = 3$. ***$P < 0.001$ vs. DMSO group.

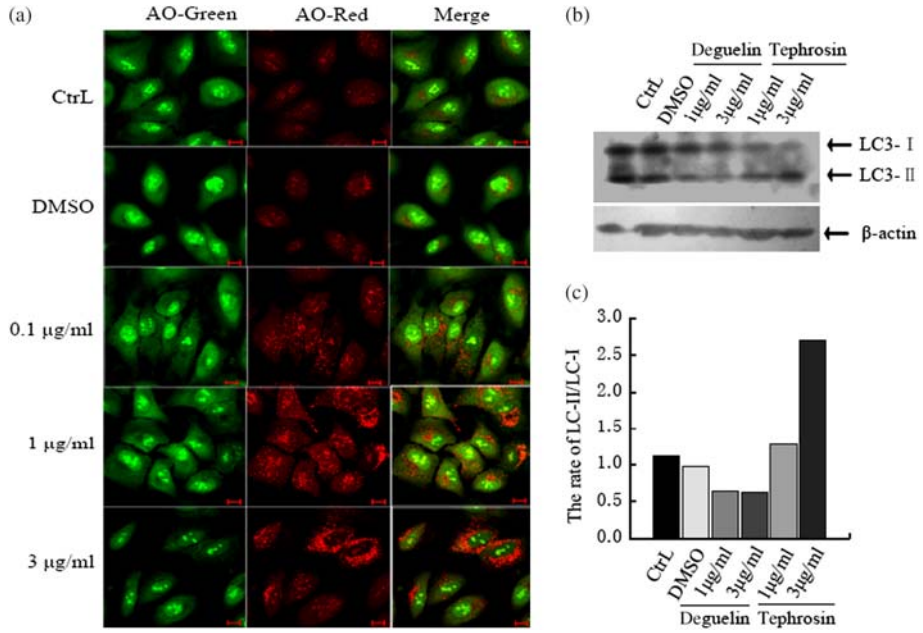

Figure 6. Tephrosin (**1**) induces A549 cell autophagy in a dose-dependent manner. (a) Representative images of A549 cells with AO-labeled vacuoles (red dots) were obtained by a confocal microscope. Scale bar: 20 μm. (b) Representative Western blotting analysis of three independent experiments. (c) Densitometric analyses of the ratio of LC3-II to LC3-I.

proteins [9]. In our study, we unexpectedly noticed that **1** resulted in the decrease in Hsp90 expression in a dose-dependent manner in A549 cancer cells (Figure 4).

2.7 Effect of 1 on the mitochondrial membrane potential of A549 cells

Mitochondria are an important regulator of autophagy-induced cell death and damaged mitochondria are often degraded by autophagosomes [10]. We therefore investigated whether **1** could induce the dissipation of the mitochondrial membrane potential of A549 cells. Figure 7 shows that the mitochondrial membrane potential obviously decreased in all **1**-treated A549 cells.

2.8 Discussion

Deguelin, another derivative of rotenone with a similar structure, has previously shown potential cancer chemopreventive efficacy against the carcinogenesis of the lung, skin, colon, and breast in several *in vitro* and *in vivo* models. In addition, deguelin was reported to inhibit the growth of different types of cancer cells by inducing apoptosis [1]. However, we observed in our experiments that **1**, also a derivative of rotenone, induced the cell cycle arrest of A549 cells significantly followed by cell death, but its mechanism probably did not involve apoptosis as no obvious PARP protein cleavage band was observed in the Western blotting experiment.

As a complex I inhibitor, rotenone induces cell death by generating ROS through the inhibition of the mitochondrial electron transport chain (mETC) [10]. Our data also demonstrated that similar to rotenone, **1** led to the ROS production obviously. It was shown that ROS produced from the mETC inhibition by rotenone

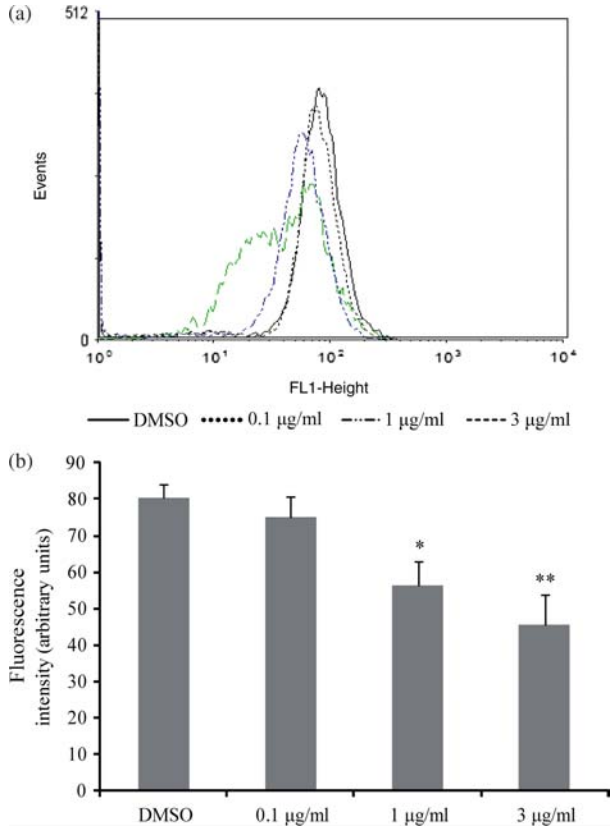

Figure 7. Changes in the mitochondrial membrane potential in A549 cells after 24 h treatment with tephrosin (**1**). (a) Representative flow cytometric analyses. (b) Statistical analyses. The values were the means ± SD. $n = 3$. $*P < 0.05$, $**P < 0.01$ vs. DMSO.

mediate autophagic cell death in transformed HEK 293 and U87 cells and apoptosis in HL60 and SH-SY5Y cells [11,12], which suggested that rotenone could induce apoptosis or autophagy in specific cell types. Here, in A549 cells, we demonstrated that **1** results significantly in autophagy other than apoptosis.

Mitochondrial transmembrane potential dissipates in autophagy to some extent induced by radiation and arsenic trioxide in malignant cells [13]. Also, another study clearly showed that superoxide anion generated selenite-triggered mitochondrial damage and subsequent autophagy, leading to irreversible cell death in cancer cells [14]. In our experiments, we also found that the mitochondrial membrane potential decreased, which may be destroyed by autophagy or by ROS directly as ROS was reported to generate oxidative damage to mitochondria. Further investigation is needed to examine the mechanism of mitochondrial damage in **1**-induced autophagy in A549 cells.

Oh [15] reported that deguelin was bound to the ATP-binding pocket of Hsp90 and disrupted Hsp90 functions. However, we noticed here that **1** treatment induced Hsp90 expression inhibition, and also no cleavage fragment of Hsp90 was found. This result indicated that the Hsp90 expression decrease was not due to be cleaved by ROS, though Beck [16]

suggested that ROS could induce Hsp90 cleavage. Hsp90-based chaperone machinery has been suggested to be important in modulating mutant CuZnSOD protein folding [17], which suggested that inhibition of Hsp90 by **1** may contribute to the ROS increase, and ROS therefore results in autophagy. In fact, Hsp90 inhibition has been reported to induce autophagy and mediate proteasome-independent degradation of IκB kinase [18], which provided the indirect evidence of the relation between Hsp90 and autophagy.

In conclusion, we have presented evidences here showing that **1** has potential anticancer activity in A549 cells, and that this beneficial effect is due to autophagy occurrence, and the roles of ROS generation and inhibition of Hsp90 expression in this process need further study in the future. Because of its relative selective cytotoxicity against different malignant cells, **1** is a promising new experimental anticancer agent for the treatment of human lung cancers.

3. Materials and methods

3.1 Cell culture

The cancer cell lines of P388 (mouse leukemia cell line), Bel7402 (human hepatoma cell line), and A549 (non-small cell lung cancer cell lines) were obtained from the Institute of Biochemistry and Cell Biology (Shanghai, China). These cancer cell lines were cultured in respective DMEM, RPMI-1640, and F12K medium supplemented with 10% fetal bovine serum and 1% penicillin–streptomycin.

3.2 Chemicals

Tetrazolium salt, 3-(4,5-dimethylthiazol-2-yl)-2,5-diphenyl-2*H*-tetrazolium bromide (MTT), propidium iodide (PI), 2′,7′-dichlorofluorescein diacetate (DCFH-DA), rhodamine 123 (Rho123), and AO were all purchased from Sigma-Aldrich, Inc. (St Louis, MO, USA). Mouse monoclonal antibodies against PARP, Hsp90, and microtubule-associated protein 1 LC3 were purchased from Santa Cruz Biotechnology, Inc. (Santa Cruz, CA, USA). The horseradish peroxidase (HRP)-conjugated goat anti-rabbit IgG and goat anti-mouse IgG were also purchased from Santa Cruz Biotechnology, Inc.

3.3 Cell viability

Cells were plated at a density of 4×10^4 cells/well in 96-well plates for 12 h, followed by treatment with **1** for a further 48 h. Cells were washed with PBS three times, and MTT (5 mg/ml) was added to the medium. The absorbance was read at 570 nm with a microplate reader (Tecan Rainbow, Groding/Salzburg, Austria).

3.4 Flow cytometric cell cycle analysis

Cells were treated at different concentrations of **1** for 12 h. The cellular DNA was stained with 200 μl of PI solution (PI: 50 μg/ml, RNase: 1 mg/ml, Triton X-100: 0.1%). After incubation at 4°C for 30 min, cells were analyzed on a flow cytometry (Becton-Dickinson, Vantage, San Jose, California, USA). Cells treated with DMSO without **1** acted as control. Data acquisition and analysis were performed using Modfit 2.0 software.

3.5 AVOs with AO staining

In brief, A549 cells were grown on glass coverslips for 24 h. After the 24 h treatment with **1**, confluent monolayers were incubated with AO (5 μg/ml) for 15–20 min. Cells were examined under a confocal laser scanning microscope (Zeiss LSM510, Jena, Germany).

3.6 Determination of ROS production

Cells treated at different concentrations of **1** for 2 and 24 h were incubated with 10 μM DCFH-DA at 37°C for 30 min,

and fluorescence intensity of DCFH-DA in A549 cells was analyzed by flow cytometry. Data acquisition and analysis were performed using Cell Quest software.

3.7 Measurement of the mitochondrial membrane potential

Briefly, 5×10^5 cells treated at different concentrations of **1** for 24 h were resuspended in 0.5 ml of ice-cold PBS, and then cultured with 1 μg/ml Rho123 in 5% CO_2 at 37°C for 15 min. The cells were analyzed by flow cytometry. Data acquisition and analysis were performed using Cell Quest software.

3.8 Western blotting assay

The cells treated with **1** for 24 h were lysed with buffer (20 mM Tris base, pH 8.0, 100 mM NaCl, 1 mM EDTA, 1 mM dithiothreitol, 1 mM Na_3VO_4, 4 μg/ml aprotinin, 1 mM phenylmethylsulfonyl fluoride (PMSF), 1% Triton X-100, 1% NP 40, 50 mM NaF) supplemented with 1 mM PMSF. Protein concentration was determined by a BCA protein assay kit. The total protein extract was separated by SDS-PAGE and transferred to a nitrocellulose membrane. After blocking with 1% BSA, membranes were incubated with antibodies against Hsp90, PARP, and LC3 proteins overnight at 4°C. Blots were washed three times in TBS-T buffer, followed by incubation with the appropriate HRP-linked secondary antibodies for 2 h. The specific proteins in the blots were visualized using the enhanced chemiluminescence reagent.

3.9 Statistical analysis

All the values were presented as means ± SD. Statistical comparisons were conducted using either one-way ANOVA for multiple comparisons or Student's *t*-test for single comparisons. Statistical significance is accepted only if $P < 0.05$.

Acknowledgements

This work was supported by the Natural Science Foundation of China (No. 30572314), the Basic Research Program of Science and Technology, Ministry of Science and Technology of China (2007FY210500), and the State Plan for High-Tech Research and Development of China (2007AA09Z405). We would like to thank Prof. Yucheng Gu from Syngenta Jealott's Hill International Research Centre for his proofreading and revision of the manuscript.

References

[1] J.K. Woo, D.S. Choi, H.T. Tran, B.E. Gilbert, W.K. Hong, and H.Y. Lee, *Cancer Prev. Res.* **2**, 361 (2009).
[2] H. Ye, L. Chen, Y. Li, A. Peng, A. Fu, H. Song, M. Tang, H. Luo, Y. Luo, Y. Xu, J. Shi, and Y. Wei, *J. Chromatogr.* **1178**, 101 (2008).
[3] F.Q. Alenzi, *Br. J. Biomed. Sci.* **61**, 99 (2004).
[4] Y. Xu, S.O. Kim, Y. Li, and J. Han, *J. Biol. Chem.* **281**, 19179 (2006).
[5] L. Yu, F. Wan, S. Dutta, S. Welsh, Z. Liu, E. Freundt, E.H. Behrecke, and M. Lenardo, *Proc. Natl. Acad. Sci. USA* **103**, 4952 (2006).
[6] P. Codogno and A.J. Meijer, *Cell Death Differ.* **12**, 1509 (2005).
[7] B. Levine and J. Yuan, *J. Clin. Invest.* **115**, 2679 (2005).
[8] F. Traganos and Z. Darzynkiewicz, *Methods Cell Biol.* **41**, 185 (1994).
[9] B.S. Blagg and T.D. Kerr, *Med. Res. Rev.* **26**, 310 (2006).
[10] Y. Chen, E. McMillan-Ward, J. Kong, S.J. Israels, and S.B. Gibson, *J. Cell Sci.* **120**, 4155 (2007).
[11] N. Li, K. Ragheb, G. Lawler, J. Sturgis, B. Rajwa, J.A. Melendez, and J.P. Robinson, *J. Biol. Chem.* **278**, 8516 (2003).
[12] K. Newhouse, S.L. Hsuan, S.H. Chang, B. Cai, Y. Wang, and Z. Xia, *Toxicol. Sci.* **79**, 137 (2004).
[13] H. Ito, S. Daido, T. Kanzawa, S. Kondo, and Y. Kondo, *Int. J. Oncol.* **26**, 1401 (2005).
[14] E.H. Kim, S. Sohn, H.J. Kwon, S.U. Kim, M.J. Kim, S.J. Lee, and K.S. Choi, *Cancer Res.* **67**, 6314 (2007).

[15] S.H. Oh, J.K. Woo, Y.D. Yazici, J.N. Myers, W.Y. Kim, Q. Jin, S.S. Hong, H.J. Park, Y.G. Suh, K.W. Kim, W.K. Hong, and H.Y. Lee, *J. Natl. Cancer Inst.* **99**, 949 (2007).

[16] R. Beck, J. Verrax, T. Gonze, M. Zappone, R.C. Pedrosa, H. Taper, O. Feron, and P.B. Calderon, *Biochem. Pharmacol.* **77**, 375 (2009).

[17] J.S. Choi, S. Cho, S.G. Park, B.C. Park, and D.H. Lee, *Biochem. Biophys. Res.* **321**, 574 (2004).

[18] G. Qing, P. Yan, and G. Xiao, *Cell Res.* **16**, 895 (2006).